

Astrometric masses of 21 asteroids, and an integrated asteroid ephemeris

James Baer · Steven R. Chesley

Received: 28 June 2007 / Revised: 14 October 2007 / Accepted: 25 October 2007 /
Published online: 18 December 2007
© Springer Science+Business Media B.V. 2007

Abstract We apply the technique of astrometric mass determination to measure the masses of 21 main-belt asteroids; the masses of 9 Metis ($1.03 \pm 0.24 \times 10^{-11} M_{\odot}$), 17 Thetis ($6.17 \pm 0.64 \times 10^{-13} M_{\odot}$), 19 Fortuna ($5.41 \pm 0.76 \times 10^{-12} M_{\odot}$), and 189 Phthia ($1.87 \pm 0.64 \times 10^{-14} M_{\odot}$) appear to be new. The resulting bulk porosities of 11 Parthenope ($12 \pm 4\%$) and 16 Psyche ($46 \pm 16\%$) are smaller than previously-reported values. Empirical expressions modeling bulk density as a function of mean radius are presented for the C and S taxonomic classes. To accurately model the forces on these asteroids during the mass determination process, we created an integrated ephemeris of the 300 large asteroids used in preparing the DE-405 planetary ephemeris; this new BC-405 integrated asteroid ephemeris also appears useful in other high-accuracy applications.

Keywords N-body · Asteroid · Ephemerides · Asteroid masses · Astrometric masses · Asteroid porosity

1 Introduction

The technique of astrometric mass determination, in which the deflection of a small body's trajectory allows us to deduce the mass of a larger perturbing body, may be entering a particularly fruitful period, as near-Earth asteroid (NEA) surveys coincidentally produce a flood of high-precision main-belt asteroid observations.

The mass of an asteroid, when combined with its volume, yields information on its composition and structure. Additionally, the inability to accurately model asteroid perturbations due to their unknown masses represents the single greatest source of error in planetary ephemerides (Standish 2000). While indirect methods of mass calculation, such as

J. Baer (✉)
South University, 1400 Penn Avenue, Pittsburgh, PA 15222, USA
e-mail: jimbaer1@earthlink.net

S. R. Chesley
Jet Propulsion Laboratory, 4800 Oak Grove Drive, Pasadena, CA 91109, USA
e-mail: steve.chesley@jpl.nasa.gov

assuming a given density based on taxonomic class, have proven extremely useful in dynamical modeling, such assumptions must be calibrated against direct observation.

In this paper, we present the astrometric masses of 21 main-belt asteroids. Their derived densities provide insight into the porosities of two asteroids, and suggest that density variations within taxonomic classes may be caused by variations in porosity. Finally, we present a fully-integrated asteroid ephemeris, compatible with the JPL DE-405 planetary ephemeris, that was developed as part of the mass determination process; and we discuss its utility for other high-precision applications.

2 Calculations: overview

Astrometric mass determination is a modification of conventional least-squares orbit determination, in which the mass of the perturbing body is added as a seventh solve-for parameter. Ideally, the process is applied to relatively close encounters between a large *subject* asteroid and a small *test* asteroid, where precise observations of the test asteroid exist before, during, and after the encounter.

Since the mass determination calculations are lengthy, it is first necessary to conduct a survey for encounters likely to result in significant deflection of the test asteroid. Furthermore, since the mass determination process is based upon perturbations in the trajectory of a test asteroid, it is absolutely essential to employ an accurate force model that accounts for all other known perturbations upon that test asteroid. And since newly-calculated asteroid masses and orbits improve the accuracy of the force model, the processes of mass determination and force model refinement are intertwined.

We will therefore begin with the selection of candidate encounters; later, we will describe the iterative scheme that yielded both the asteroid masses and the asteroid ephemeris.

2.1 Selection of candidate encounters

As described by [Michalak \(2000\)](#), perhaps the most direct method of selecting suitable mass determination encounters involves integrating the orbit of a small test asteroid through the period of available observations, both with and without the influence of the large subject asteroid; cases in which the perturbed and unperturbed trajectories result in significant differences in predicted right ascension and declination are obvious candidates for detailed analysis.

However, with over 120,000 numbered asteroids catalogued at the time of our analysis, we felt that the integration required to test all of the possible encounters for even a limited number of large asteroids would be prohibitive. We therefore sought a computationally-efficient alternative.

A two-body approximation of the deflection angle θ in the trajectory of a small test asteroid due to the gravitational perturbation of an encounter with a large subject asteroid is given by

$$\tan \frac{\theta}{2} = \frac{G(m + M)}{v^2 b}$$

where m and M represent the masses of the test and subject asteroids, v is the unperturbed relative velocity, and b is the unperturbed distance of closest approach.

However, there are limits to relying solely upon the deflection angle as the survey criterion. First, it is unclear whether the direction of deflection will result in an easily-observable change in trajectory; a deflection that largely impacts the inclination of the test asteroid's orbit, for instance, would not be as easily noted as a deflection that significantly alters its semi-major

axis. Second, even a relatively small change in the test asteroid's semi-major axis may provide useful data if several decades of observations exist both before and after the encounter.

In hopes of optimizing our selection of candidate encounters, we therefore applied Öpik's two-body analysis of planetary encounters, as developed by Carusi et al. (1990) and Valsecchi et al. (2003). This two-body analysis allowed us to estimate the change in the inclination and semi-major axis of a test asteroid's orbit due to an encounter with a larger subject asteroid. Thus, for each large subject asteroid, we tested every other possible numbered test asteroid in the Minor Planet Center orbital database (MPCORB) with a relative Minimum Orbital Intersection Distance (MOID) of 0.1 AU or less, conservatively selecting those encounters within the period of observation of the test asteroid resulting in a predicted deflection angle, predicted change in inclination, or predicted change in sky position, exceeding 0.002 arcseconds. In total, over 2,500 candidate events were identified.

2.2 The force model

The main asteroid belt is a chaotic system in which each asteroid is gravitationally perturbing every other asteroid; to make an analogy with radio, successful mass determination therefore requires isolating a very weak signal from a very noisy background environment. Clearly, we needed to account for every other significant perturbation on a test asteroid, so that the perturbations due to the subject asteroid could be isolated by the least-squares algorithm.

The software used for the mass determinations was a modified version of the CODES application (Baer 2004), whose integration force model accounts for gravitational perturbations (including first-order relativistic terms), the oblateness of the Sun, Earth, and Jupiter, and solar radiation pressure. In calculating gravitational perturbations due to the Sun, planets, and Earth's Moon, CODES uses the JPL DE-405 ephemeris, which provides precise positions of these bodies for the period 1800–2200.

Standish explains that, in accounting for perturbations due to the 300 most important perturbing asteroids, the DE-403 ephemeris calculated positions of these asteroids using their mean orbital elements (Standish et al. 1995). The masses of these perturbing asteroids were modeled using IRAS diameters, assuming a uniform density for asteroids of each taxonomic class (the respective class densities were adjusted as part of the least-squares solution). In refining this process for DE-405, the orbits of Ceres, Pallas, and Vesta (CPV) were integrated accounting for perturbations from the Sun, planets, and Moon, while the orbits of the other 297 asteroids were integrated accounting for perturbations from the Sun, planets, Moon, Ceres, Pallas, and Vesta (Standish 1998).

The baseline CODES application used an approach similar to DE-403, accounting for gravitational perturbations from the 300 asteroids based on positions from mean orbital elements. Clearly, such an approximation would not suffice here.

To enhance the CODES force model for mass determination, we therefore resolved to create a fully-integrated ephemeris of the 300 asteroids, in which the orbit of each asteroid would account for perturbations from the Sun, planets, Earth's Moon, and the other 299 asteroids. Since this ephemeris, covering the timeframe 1800–2200, would be derived from (and fully consistent with) DE-405, we termed it the BC-405 asteroid ephemeris.

2.3 The iterative process

Clearly, the masses of the 300 asteroids would be required to model their perturbations; but since the entire purpose of the BC-405 ephemeris was to facilitate the determination of those very same masses, we decided to pursue an iterative approach.

First, we applied the mass determination algorithm to the 2,500+ candidate encounters, using a simplified “CPV-only” asteroid ephemeris, with the CPV masses taken from DE-405 and the CPV orbits based on mean elements. Measured masses were considered valid if they yielded a density of between 0.5 and 8.0 g/cm³, and if the *significance* (defined as the ratio of the measured mass to its formal uncertainty) exceeded two. Only those 102 candidate events (involving 21 asteroids) resulting in valid masses, or in mass uncertainties less than one-half of the a priori mass (estimated using a density of 2 g/cm³ and the known IRAS diameter), were retained for further study.

An initial *draft zero* version of the BC-405 ephemeris was then created, using MPCORB state vectors (Marsden 2005) of the 300 asteroids at epoch, the best available published masses (see Table 1) for some of the largest asteroids, and estimates based on DE-403 taxonomic class densities (see Table 2) and IRAS diameters (Tedesco et al. 2002) for the masses of all other asteroids. This draft zero ephemeris was used by the mass determination algorithm to analyze the remaining 102 candidate events, using all available observations of the test asteroids in the AstDyS database (Milani and Chesley 1999). The draft zero ephemeris, with the draft zero asteroid masses, was also used in a conventional orbit determination algorithm to refine the epoch state vectors of the 300 asteroids in the ephemeris, using all available observations of each ephemeris asteroid in the AstDyS database.

With the first iteration complete, the newly-recalculated masses and refined state vectors were used to create the second version of the ephemeris; as before, this version of the ephemeris was then used to recalculate the masses and refine the ephemeris state vectors. The entire process was repeated four times, by which point 1,792 of the 1,800 state vector components in successive versions of the ephemeris agreed to within 0.1σ , and the other eight state vector components agreed to within 1σ .

The final result was an internally-consistent set of measured masses and ephemeris state vectors.

This iterative approach does not reveal pathologies such as high correlations among the solve-for parameters; and it does not immediately guarantee convergence to a global minimum solution. However, aside from the CPV perturbations (which are well-determined from a variety of sources), the force model modifications associated with the masses of the other 297 asteroids have a relatively slight effect on the global solution; and no convergence issues were apparent. Moreover, the selected initial mass values are unlikely to be off by more than a factor of three, which argues a priori for only modest corrections to both state and mass parameter values. Still, errors in the assumed masses of the 279 asteroid masses for which we did not solve could bias the 21 estimated masses. Future revisions to this work may allow more insight into the significance of such concerns.

Note: Radar observations exist for only 11 of the 300 ephemeris asteroids, comprising 26 total observations. Thus, while such observations are highly-precise, no attempt was made to analyze their relative impact on the state vector solutions.

2.4 The mass determination algorithm

As noted above, the mass determination algorithm consists of calculating a precise orbit of the test asteroid, and solving for the perturbing mass of the subject asteroid. To provide context for what follows, we will briefly review the orbit determination process.

The conventional least-squares orbit determination algorithm relies upon finding the minimum of the cost function

$$Q(x) = b^T \Lambda^{-1} b$$

Table 1 Recent asteroid mass determinations

Asteroid	Mass (in M_{\odot})	References
1 Ceres	$4.7 \pm 0.3 \times 10^{-10}$	Goffin (1991)
	$4.796 \pm 0.085 \times 10^{-10}$	Sitarski and Todorovic-Juchniewicz (1992)
	$4.80 \pm 0.22 \times 10^{-10}$	Williams (1992)
	$4.622 \pm 0.071 \times 10^{-10}$	Sitarski and Todorovic-Juchniewicz (1995)
	$5.0 \pm 0.2 \times 10^{-10}$	Viateau and Rapaport (1995)
	$4.67 \pm 0.09 \times 10^{-10}$	Carpino and Knezevic (1996)
	$4.16 \pm 0.19 \times 10^{-10}$	Kuzmanoski (1996)
	$4.785 \pm 0.039 \times 10^{-10}$	Viateau and Rapaport (1997a)
	$4.759 \pm 0.023 \times 10^{-10}$	Viateau and Rapaport (1998)
	$4.39 \pm 0.04 \times 10^{-10}$	Hilton (1999)
	$4.70 \pm 0.04 \times 10^{-10}$	Michalak (2000)
	$4.762 \pm 0.015 \times 10^{-10}$	Standish (2001)
	$4.81 \pm 0.01 \times 10^{-10}$	Pitjeva (2001)
	$4.749 \pm 0.020 \times 10^{-10}$	Pitjeva (2004)
	$4.753 \pm 0.007 \times 10^{-10}$	Pitjeva (2005)
	$4.699 \pm 0.028 \times 10^{-10}$	Konopliv et al. (2006)
$4.75 \pm 0.03 \times 10^{-10}$	Table 3	
2 Pallas	$1.59 \pm 0.05 \times 10^{-10}$	Hilton (1999)
	$1.21 \pm 0.26 \times 10^{-10}$	Michalak (2000)
	$1.17 \pm 0.03 \times 10^{-10}$	Goffin (2001)
	$1.078 \pm 0.038 \times 10^{-10}$	Standish (2001)
	$1.00 \pm 0.01 \times 10^{-10}$	Pitjeva (2001)
	$1.036 \pm 0.02 \times 10^{-10}$	Pitjeva (2004)
	$1.027 \pm 0.003 \times 10^{-10}$	Pitjeva (2005)
	$1.026 \pm 0.028 \times 10^{-10}$	Konopliv et al. (2006)
$1.06 \pm 0.13 \times 10^{-10}$	Table 3	
3 Juno	$2.09 \pm 0.35 \times 10^{-11}$	Chernetenko and Kochetova (2002)
	$1.42 \pm 0.06 \times 10^{-11}$	Pitjeva (2004)
	$1.51 \pm 0.03 \times 10^{-11}$	Pitjeva (2005)
	$1.49 \pm 0.15 \times 10^{-11}$	Konopliv et al. (2006)
4 Vesta	$1.396 \pm 0.043 \times 10^{-10}$	Sitarski and Todorovic-Juchniewicz (1995)
	$1.69 \pm 0.05 \times 10^{-10}$	Hilton (1999)
	$1.36 \pm 0.05 \times 10^{-10}$	Michalak (2000)
	$1.306 \pm 0.016 \times 10^{-10}$	Viateau and Rapaport (2001)
	$1.341 \pm 0.015 \times 10^{-10}$	Standish (2001)
	$1.36 \pm 0.01 \times 10^{-10}$	Pitjeva (2001)
	$1.38 \pm 0.03 \times 10^{-10}$	Konopliv (personal communication)
	$1.358 \pm 0.02 \times 10^{-10}$	Pitjeva (2004)
	$1.344 \pm 0.001 \times 10^{-10}$	Pitjeva (2005)
	$1.358 \pm 0.016 \times 10^{-10}$	Konopliv et al. (2006)
	$1.34 \pm 0.01 \times 10^{-10}$	Table 3
	$6.9 \pm 2.2 \times 10^{-12}$	Michalak (2001)
6 Hebe	$7.59 \pm 1.42 \times 10^{-12}$	Table 3
		Chernetenko and Kochetova (2002)
7 Iris	$1.41 \pm 0.14 \times 10^{-11}$	Pitjeva (2004)
	$5.2 \pm 0.8 \times 10^{-12}$	Pitjeva (2005)
	$6.3 \pm 0.1 \times 10^{-12}$	Table 3
	$6.81 \pm 1.93 \times 10^{-12}$	Table 3
9 Metis	$1.03 \pm 0.24 \times 10^{-11}$	Table 3
10 Hygiea	$5.57 \pm 0.70 \times 10^{-11}$	Michalak (2001)
	$5.01 \pm 0.41 \times 10^{-11}$	Chernetenko and Kochetova (2002)
	$4.54 \pm 0.13 \times 10^{-11}$	Chesley et al. (2005)
	$4.54 \pm 0.15 \times 10^{-11}$	Table 3

Table 1 continued

Asteroid	Mass (in M_{\odot})	References
11 Parthenope	$2.58 \pm 0.10 \times 10^{-12}$	Viateau and Rapaport (1997b)
	$2.56 \pm 0.07 \times 10^{-12}$	Viateau and Rapaport (2001)
	$3.16 \pm 0.06 \times 10^{-12}$	Table 3
15 Eunomia	$1.26 \pm 0.30 \times 10^{-11}$	Michalak (2001)
	$1.22 \pm 0.16 \times 10^{-11}$	Chernetenko and Kochetova (2002)
	$1.64 \pm 0.06 \times 10^{-11}$	Vitagliano and Stoss (2006)
	$1.68 \pm 0.08 \times 10^{-11}$	Table 3
16 Psyche	$0.87 \pm 0.26 \times 10^{-11}$	Viateau (2000)
	$3.38 \pm 0.28 \times 10^{-11}$	Kuzmanoski and Kovačević (2002)
	$1.29 \pm 0.17 \times 10^{-11}$	Table 3
17 Thetis	$6.17 \pm 0.64 \times 10^{-13}$	Table 3
19 Fortuna	$5.41 \pm 0.76 \times 10^{-12}$	Table 3
20 Massalia	$2.42 \pm 0.41 \times 10^{-12}$	Bange (1998)
24 Themis	$2.89 \pm 1.26 \times 10^{-12}$	Lopez Garcia et al. (1997)
	$5.67 \pm 2.15 \times 10^{-12}$	Table 3
29 Amphitrite	$0.77 \pm 0.12 \times 10^{-11}$	Chernetenko and Kochetova (2002)
	$1.00 \pm 0.35 \times 10^{-11}$	Table 3
45 Eugenia	$3.0 \pm 0.1 \times 10^{-12}$	Merline et al. (1999)
46 Hestia	$1.09 \pm 0.68 \times 10^{-11}$	Bange and Bec-Borsenberger (1997)
52 Europa	$2.61 \pm 0.88 \times 10^{-11}$	Michalak (2001)
	$1.28 \pm 0.25 \times 10^{-11}$	Chernetenko and Kochetova (2002)
	$9.76 \pm 2.21 \times 10^{-12}$	Table 3
65 Cybele	$5.8 \pm 1.5 \times 10^{-12}$	Chernetenko and Kochetova (2002)
	$7.59 \pm 1.82 \times 10^{-12}$	Table 3
87 Sylvia	$7.6 \pm 0.8 \times 10^{-12}$	Margot and Brown (2001)
	$7.431 \pm 0.030 \times 10^{-12}$	Marchis et al. (2005)
88 Thisbe	$7.4 \pm 1.3 \times 10^{-12}$	Michalak (2001)
	$5.72 \pm 1.76 \times 10^{-12}$	Table 3
	$4.14 \pm 0.05 \times 10^{-13}$	Merline et al. (2002)
121 Hermione	$4.7 \pm 0.8 \times 10^{-12}$	Viateau (2000)
189 Phthia	$1.87 \pm 0.64 \times 10^{-14}$	Table 3
243 Ida	$1.92 \pm 0.09 \times 10^{-14}$	Petit et al. (1997)
253 Mathilde	$5.19 \pm 0.22 \times 10^{-14}$	Yeomans et al. (1997)
324 Bamberga	$5.1 \pm 0.8 \times 10^{-12}$	Pitjeva (2004)
	$5.5 \pm 0.1 \times 10^{-12}$	Pitjeva (2005)
	$4.7 \pm 0.7 \times 10^{-12}$	Konopliv et al. (2006)
	$3.362 \pm 0.002 \times 10^{-15}$	Yeomans et al. (2000)
433 Eros	$3.6 \pm 1.6 \times 10^{-12}$	Michalak (2001)
444 Gypsis	$3.34 \pm 0.28 \times 10^{-11}$	Michalak (2001)
	$2.40 \pm 0.24 \times 10^{-11}$	Chernetenko and Kochetova (2002)
	$2.98 \pm 0.30 \times 10^{-11}$	Table 3
704 Interamnia	$3.7 \pm 1.7 \times 10^{-11}$	Landgraff (1992)
	$3.52 \pm 0.93 \times 10^{-11}$	Michalak (2001)
	$0.81 \pm 0.42 \times 10^{-11}$	Chernetenko and Kochetova (2002)
	$3.58 \pm 0.42 \times 10^{-11}$	Table 3
762 Pulcova	$1.3 \pm 0.2 \times 10^{-12}$	Merline et al. (2002)
804 Hispania	$5 \pm 4 \times 10^{-12}$	Landgraff (1992)
	$4.69 \pm 1.85 \times 10^{-12}$	Table 3
1999 KW4	$1.1 \pm 0.1 \times 10^{-18}$	Margot et al. (2002)
2000 DP107	$2.3 \pm 0.4 \times 10^{-19}$	Margot et al. (2002)
2000 UG11	$4.7 \pm 0.8 \times 10^{-21}$	Margot et al. (2002)
2002 CE26	$9.8 \pm 1.3 \times 10^{-18}$	Shepard et al. (2006)

Table 2 Bulk densities for taxonomic classes

Taxonomic class	Bulk density (g/cm ³)			
	This paper	DE-403	Standish (2001)	Krasinsky et al. (2002)
C	2.09	1.80	1.29	1.38
S	2.75	2.40	2.71	2.71
M	4.02	5.00	5.29	5.32

In this equation, x is the state vector, $b = b(x)$ is a vector containing the “observed-computed” residuals for each observation, and Λ is the observational covariance matrix, with

$$\Lambda_{ij} = r_{ij}\sigma_i\sigma_j$$

where σ_i is the square root of the covariance of the i th observation, and r_{ij} is the correlation between the i th and j th observations. We would find the minimum by seeking stationary points of $Q(x)$:

$$0 = \frac{dQ}{dx} = 2b^T \Lambda^{-1} \frac{db}{dx}$$

If we define $A = \frac{db}{dx}$, then the equation to be solved reduces to

$$0 = A^T \Lambda^{-1} b$$

If we assume a total of N data points, where $N = 2(\text{number of optical observations}) + (\text{number of radar delay observations}) + (\text{number of radar doppler observations})$, then b is an $N \times 1$ vector, and A is an $N \times 6$ matrix.

The solution of this equation is

$$dx = -(A^T \Lambda^{-1} A)^{-1} A^T \Lambda^{-1} b$$

Conventionally, it is assumed that σ_i is 3 arcseconds for optical observations prior to 1,890, 2 arcseconds for observations from 1890 to 1950, and 1 arcsecond thereafter. The additional assumption that observations are uncorrelated, i.e.,

$$r_{ij} = \begin{cases} 1 & \text{when } i = j, \\ 0 & \text{when } i \neq j \end{cases}$$

leads to Λ being a diagonal matrix. The validity and consequences of these assumptions will be addressed in the final section of this paper.

The CODES least squares algorithm uses an outlier rejection strategy similar to that described by [Carpino et al. \(2003\)](#). In the initial stages, all available optical and radar observations of the test asteroid are used, until successive state vector solutions converge. Then observations with χ^2 values exceeding a user-defined threshold χ_{lim}^2 are excluded, and a new solution is calculated, with the process being repeated until successive state vector solutions again converge; in each successive solution, every observation is considered for inclusion, even if it had been excluded in the prior solution.

In modifying this algorithm for astrometric mass determination, the mass of the perturbing subject asteroid was added as a seventh solve-for parameter in Δx ; determining the orbit of the test asteroid in each encounter therefore also determined the mass of the subject asteroid.

Since no manual editing of observations would be used, we decided to attempt to duplicate the effect of such editing through control of the χ_{lim}^2 threshold. First, the masses were calculated using a threshold of $\chi_{lim}^2 = 25$. The resulting subject asteroid mass and test asteroid

state vector were then used to initialize a second mass determination using a threshold of $\chi_{\text{lim}}^2 = 9$. Finally, the resulting subject asteroid mass and test asteroid state vector were used to initialize a third mass determination using a threshold of $\chi_{\text{lim}}^2 = 2.25$. The solution with the highest significance was selected.

In addition to the 300 asteroids in the BC-405 ephemeris, the mass determination force model also accounted for perturbations from any other asteroids that our survey predicted might deflect the test asteroid. The trajectories of these *additional perturbers* were integrated using CPV propagation, beginning with the MPCORB epoch state vector; and since published masses for these additional perturbers were not available, their masses were estimated using taxonomic class-based densities and IRAS diameters.

For asteroids 10 Hygiea, 15 Eunomia, 16 Psyche, 52 Europa, 87 Sylvia, 511 Davida, and 704 Interamnia, parallel mass determinations were made by an independent software set (Chesley et al. 2005); agreement between the two algorithms was excellent, and the results with the largest significance were used.

3 Results

In all, 56 of the candidate events yielded valid masses. Any measured masses differing from the weighted average for that asteroid by more than 6σ were discarded. In the cases of asteroids 1 Ceres, 4 Vesta, and 10 Hygiea, literally dozens of valid masses were obtained; but to optimize the quality of the results, only those events where the significance exceeded a given threshold (50 for Ceres and Vesta, 30 for Hygiea) were used.

Our resulting individual mass determination events and weighted averages are listed in Table 3; the weighted averages are also listed in Table 1 alongside other recently published values.

Of the 21 asteroids for which valid masses were measured, 4 masses appear to be new, 16 agree to within 1σ with previously published values, and 1 agrees to within 2σ of previously published values.

Using the best available dimensions for each asteroid, Table 3 also lists the derived bulk densities; note that the uncertainties in bulk density account for uncertainties in both mass and volume.

Table 3 Mass/density determinations and weighted averages

Subject ast	Test ast	Mass (M_{\odot})	Significance	Bulk density (g/cm^3)	Tax class	Dimensions (km)	Δr (km)
1	348	$4.76 \pm 0.06 \times 10^{-10}$	86.1	2.09 ± 0.05	G ^j	$975 \times 975 \times 909^a$	3.6^a
1	5303	$4.76 \pm 0.05 \times 10^{-10}$	95.2	2.10 ± 0.05	G ^j	$975 \times 975 \times 909^a$	3.6^a
1	91	$4.70 \pm 0.07 \times 10^{-10}$	70.0	2.07 ± 0.05	G ^j	$975 \times 975 \times 909^a$	3.6^a
<i>Weighted avg.</i>		$4.75 \pm 0.03 \times 10^{-10}$		2.09 ± 0.05			
2	5930	$1.28 \pm 0.40 \times 10^{-10}$	3.2	3.25 ± 1.02	B	$570 \times 525 \times 500^b$	3^b
2	3131	$8.35 \pm 3.75 \times 10^{-11}$	2.2	2.12 ± 0.96	B	$570 \times 525 \times 500^b$	3^b
2	4971	$1.78 \pm 0.68 \times 10^{-10}$	2.6	4.53 ± 1.75	B	$570 \times 525 \times 500^b$	3^b
2	582	$1.03 \pm 0.15 \times 10^{-10}$	6.8	2.62 ± 0.39	B	$570 \times 525 \times 500^b$	3^b
<i>Weighted avg.</i>		$1.06 \pm 0.13 \times 10^{-10}$		2.70 ± 0.34			
4	17	$1.33 \pm 0.01 \times 10^{-10}$	94.0	3.42 ± 0.20	V	$578 \times 560 \times 458^c$	5^c
4	197	$1.34 \pm 0.03 \times 10^{-10}$	46.1	3.43 ± 0.21	V	$578 \times 560 \times 458^c$	5^c
<i>Weighted avg.</i>		$1.34 \pm 0.01 \times 10^{-10}$		3.42 ± 0.20			
6	5295	$11.74 \pm 4.44 \times 10^{-12}$	2.6	6.92 ± 3.30	S	$205 \times 185 \times 170^{d,e}$	9^e

Table 3 continued

Subject ast	Test ast	Mass (M_{\odot})	Significance	Bulk density (g/cm^3)	Tax class	Dimensions (km)	Δr (km)
6	4497	$7.87 \pm 2.01 \times 10^{-12}$	3.9	4.64 ± 1.79	S	$205 \times 185 \times 170^{\text{d,e}}$	9^{e}
6	1150	$6.13 \pm 2.27 \times 10^{-12}$	2.7	3.62 ± 1.70	S	$205 \times 185 \times 170^{\text{d,e}}$	9^{e}
<i>Weighted avg.</i>		$7.59 \pm 1.42 \times 10^{-12}$		4.47 ± 1.55			
7	17186	$6.81 \pm 1.93 \times 10^{-12}$	3.5	3.18 ± 1.31	S	$225 \times 190 \times 190^{\text{e,f}}$	10^{e}
9	43432	$1.10 \pm 0.37 \times 10^{-11}$	3.0	6.51 ± 3.33	S	$235 \times 195 \times 140^{\text{d,g,h}}$	12^{e}
9	20	$0.98 \pm 0.31 \times 10^{-11}$	3.1	5.81 ± 2.92	S	$235 \times 195 \times 140^{\text{d,g,h}}$	12^{e}
<i>Weighted avg.</i>		$1.03 \pm 0.24 \times 10^{-11}$		6.11 ± 2.76			
10	3946	$4.54 \pm 0.15 \times 10^{-11}$	30.3	2.56 ± 0.76	C	$500 \times 385 \times 350^{\text{e,f}}$	20^{e}
11	17	$3.16 \pm 0.06 \times 10^{-12}$	56.2	3.33 ± 1.04	S	$153 \times 153 \times 153^{\text{e}}$	8^{e}
15	1284	$1.88 \pm 0.35 \times 10^{-11}$	5.4	4.30 ± 1.54	S	$330 \times 245 \times 205^{\text{e,f}}$	13^{e}
15	50278	$1.67 \pm 0.09 \times 10^{-11}$	18.9	3.81 ± 1.18	S	$330 \times 245 \times 205^{\text{e,f}}$	13^{e}
<i>Weighted avg.</i>		$1.68 \pm 0.08 \times 10^{-11}$		3.85 ± 1.19			
16	13206	$1.36 \pm 0.20 \times 10^{-11}$	6.9	4.23 ± 1.46	M	$280 \times 230 \times 190^{\text{e,f}}$	12^{e}
16	94	$1.08 \pm 0.35 \times 10^{-11}$	3.1	3.35 ± 1.51	M	$280 \times 230 \times 190^{\text{e,f}}$	12^{e}
<i>Weighted avg.</i>		$1.29 \pm 0.17 \times 10^{-11}$		4.02 ± 1.36			
17	11	$6.17 \pm 0.64 \times 10^{-13}$	9.6	3.21 ± 0.92	S	$90 \times 90 \times 90^{\text{e}}$	4^{e}
19	3486	$4.46 \pm 1.32 \times 10^{-12}$	3.4	1.49 ± 0.62	G ^j	$225 \times 225 \times 225^{\text{e}}$	11^{e}
19	135	$5.88 \pm 0.93 \times 10^{-12}$	6.3	1.96 ± 0.65	G ^j	$225 \times 225 \times 225^{\text{e}}$	11^{e}
<i>Weighted avg.</i>		$5.41 \pm 0.76 \times 10^{-12}$		1.80 ± 0.59			
24	2296	$5.67 \pm 2.15 \times 10^{-12}$	2.6	2.78 ± 1.35	C	$198 \times 198 \times 198^{\text{e}}$	10^{e}
29	48464	$1.00 \pm 0.35 \times 10^{-11}$	2.9	3.99 ± 1.85	S	$212 \times 212 \times 212^{\text{e}}$	11^{e}
52	124	$10.04 \pm 3.74 \times 10^{-12}$	2.7	1.40 ± 0.67	CF	$360 \times 315 \times 240^{\text{e,i}}$	15^{e}
52	306	$9.61 \pm 2.73 \times 10^{-12}$	3.5	1.34 ± 0.56	CF	$360 \times 315 \times 240^{\text{e,i}}$	15^{e}
<i>Weighted avg.</i>		$9.76 \pm 2.21 \times 10^{-12}$		1.36 ± 0.51			
65	526	$7.59 \pm 1.82 \times 10^{-12}$	4.2	2.16 ± 0.83	P	$237 \times 237 \times 237^{\text{e}}$	12^{e}
88	7	$5.09 \pm 1.87 \times 10^{-12}$	2.7	2.40 ± 1.14	CF	$201 \times 201 \times 201^{\text{e}}$	10^{e}
88	7629	$10.56 \pm 5.20 \times 10^{-12}$	2.0	4.97 ± 2.87	CF	$201 \times 201 \times 201^{\text{e}}$	10^{e}
<i>Weighted avg.</i>		$5.72 \pm 1.76 \times 10^{-12}$		2.69 ± 1.16			
189	6224	$1.87 \pm 0.64 \times 10^{-14}$	2.9	1.33 ± 0.62	S	$38 \times 38 \times 38^{\text{e}}$	2^{e}
511	532	$2.90 \pm 0.35 \times 10^{-11}$	8.2	3.18 ± 1.03	C	$326 \times 326 \times 326^{\text{e}}$	16^{e}
511	1550	$3.18 \pm 0.56 \times 10^{-11}$	5.6	3.48 ± 1.21	C	$326 \times 326 \times 326^{\text{e}}$	16^{e}
<i>Weighted avg.</i>		$2.98 \pm 0.30 \times 10^{-11}$		3.27 ± 1.02			
704	95	$3.36 \pm 0.66 \times 10^{-11}$	5.1	4.03 ± 1.45	F	$316 \times 316 \times 316^{\text{e}}$	16^{e}
704	7461	$1.84 \pm 0.77 \times 10^{-11}$	2.4	2.20 ± 1.13	F	$316 \times 316 \times 316^{\text{e}}$	16^{e}
704	10034	$5.79 \pm 1.00 \times 10^{-11}$	5.8	6.93 ± 2.42	F	$316 \times 316 \times 316^{\text{e}}$	16^{e}
704	37	$5.35 \pm 1.18 \times 10^{-11}$	4.5	6.41 ± 2.40	F	$316 \times 316 \times 316^{\text{e}}$	16^{e}
<i>Weighted avg.</i>		$3.58 \pm 0.42 \times 10^{-11}$		4.29 ± 1.39			
804	1002	$4.69 \pm 1.85 \times 10^{-12}$	2.5	4.55 ± 2.27	P	$158 \times 158 \times 158^{\text{e}}$	8^{e}

References:^a Thomas et al. (2005); ^b Dunham et al. (1990); ^c Thomas et al. (1997); ^d Torppa et al. (2003); ^e Tedesco et al. (2002); ^f Kaasalainen et al. (2002); ^g Kissling et al. (1991); ^h Storrs et al. (2005); ⁱ Michałowski et al. (2004); ^j Neese (2005)

4 Discussion

While the asteroid masses and ephemeris are of obvious interest in astrodynamics, the derived bulk densities can provide information on porosity, which also leads to results relevant to astrodynamical modeling. Note, for instance, that the densities in Table 3 of 189 Phthia and 29 Amphitrite differ by a factor of three, despite the fact that they are both S-class asteroids.

Similarly, the densities of 52 Europa and 88 Thisbe differ by a factor of two, despite both being C-class asteroids. Such variations in density within a single taxonomic class are inconsistent with the typical assumption that class densities are uniform.

4.1 Porosity

As explained by [Britt et al. \(2002\)](#), most asteroids are not solid rock; instead, they contain macroscopic voids. Thus, the calculated bulk density (total mass divided by total volume) may be lower than the grain density of the constituent minerals. This has significant implications for disrupting a threatening near-Earth asteroid, since highly-porous asteroids attenuate impact shocks more efficiently than solid asteroids, with much of the impact energy being expended in collapsing the voids.

If we can determine the primary constituent minerals from spectroscopic analysis, the bulk porosity n of an asteroid can be calculated as

$$n = 1 - \frac{\rho}{\rho_g}$$

where ρ is the bulk density, and ρ_g is the grain density, or the density of a solid mineral with no voids.

For instance, 16 Psyche is an M-class asteroid believed to be composed of nickel–iron (Ni/Fe), for which the grain density is approximately 7.4 g/cm^3 . Given a calculated bulk density from [Table 3](#) of $4.02 \pm 1.36 \text{ g/cm}^3$, the bulk porosity is $46 \pm 16\%$. Note that this is less than the 73% bulk porosity calculated by [Britt et al. \(2002\)](#), based on a previous mass estimate. Similarly, 11 Parthenope is an S-class asteroid believed composed of silicates such as pyroxene and olivine, for which the grain density is approximately 3.8 g/cm^3 . Given a calculated bulk density from [Table 3](#) of $3.33 \pm 1.04 \text{ g/cm}^3$, the bulk porosity is $12 \pm 4\%$, again smaller than the 28% calculated by [Britt et al. \(2002\)](#) based on a previous mass estimate.

4.2 Asteroid mean radius vs. bulk density

[Table 2](#) indicates that the mean C- and S-class densities obtained from our 21 mass estimates of large asteroids were significantly higher than the class densities derived in ephemeris development, where all asteroids of a given class are assumed to have a uniform bulk density. Since our mass determination survey was intentionally centered on the largest asteroids, and since we observed non-uniform densities within taxonomic classes, we investigated whether there might be a relationship between asteroid radius and bulk density.

[Figures 1 and 2](#) include all of the C- and S-class asteroids from [Table 1](#); the correlation coefficients of 0.55 for the data in [Fig. 1](#) and 0.68 for the data in [Fig. 2](#) suggest a fairly strong relationship between mean radius and bulk density. The best-fit line for C-class is

$$\rho = 1.3866 + 0.0065 \times r$$

while the best-fit line for S-class is

$$\rho = 2.0310 + 0.0205 \times r$$

where the bulk density ρ is expressed in g/cm^3 , and the mean radius r is expressed in km.

Note that the best-fit line in [Fig. 1](#) predicts that large C-class asteroids should have bulk densities of approximately 3 g/cm^3 , while the best-fit line in [Fig. 2](#) predicts that large S-class asteroids should have bulk densities of approximately 4 g/cm^3 . These are similar to

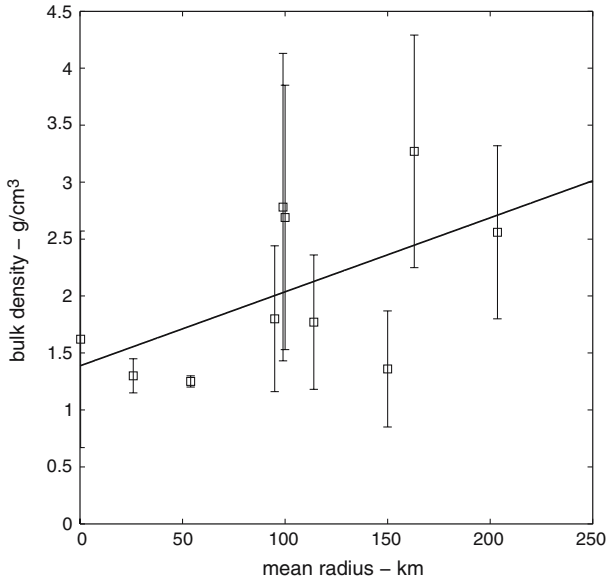


Fig. 1 Mean radius versus bulk density for C-class asteroids

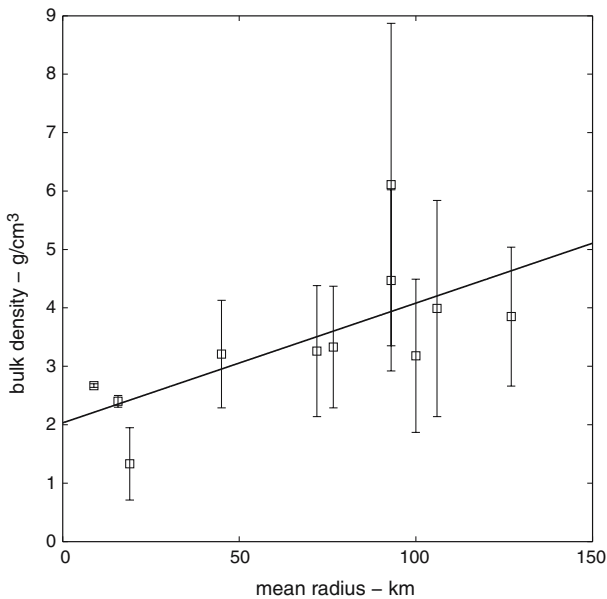


Fig. 2 Mean radius versus bulk density for S-class asteroids

the grain densities of analogous meteorites (Britt et al. 2002). In each figure, however, as the mean radius is reduced, corresponding reductions in bulk density suggest increasing levels of porosity.

One possible explanation might be that, while most asteroids began as relatively solid objects with low porosity, subsequent collisions have resulted in varying degrees of structural change. We would expect the largest asteroids to survive most impacts with little damage;

their bulk densities should therefore remain similar to the grain densities of their constituent minerals. But medium-sized asteroids might develop fractures; and the resulting voids would result in a moderate degree of porosity, and a reduced bulk density. The smaller asteroids might suffer catastrophic damage, even to the point of disruption; the fragments would subsequently collapse under their own weak gravitational attraction, leaving extensive voids between them. Such “rubble piles” would have high porosity, and low bulk density.

This rough model cannot precisely account for the structural evolution of every C- or S-class asteroid. Some medium-sized asteroids, such as 52 Europa, 90 Antiope and 189 Phthia, may also have suffered particularly severe collisions, resulting in high levels of porosity that leave them below the trend lines.

Nevertheless, in modeling the masses of C- and S-class asteroids in ephemerides and astrodynamical simulations, we would suggest that these linear “mean radius versus bulk density” relations may yield a better approximation than the current uniform class densities.

4.3 Asteroid ephemeris applications

The BC-405 ephemeris has been integrated into the most recent version of CODES, and is freely available for download from the CODES website (Baer 2004). Explanation of the structure of the ephemeris is provided, so it could easily be adapted for use in other software packages.

Table 4 illustrates that the BC-405 epoch state vector for 1 Ceres appears to offer a significant improvement in accuracy, compared to the state vector on Horizons (Giorgini et al. 1999). These improvements are consistent for the other asteroids in the ephemeris, and presumably reflect the use of a more accurate force model in the orbit determination process.

Such benefits are not restricted to the 300 asteroids in the ephemeris itself. Table 5 illustrates similar improvements in trajectory propagation for a hypothetical intercept of NEA

Table 4 Comparison of 1 Ceres orbital elements (Epoch = JD 2453775.0, heliocentric ecliptic reference frame)

	CODES & BC-405		JPL horizons & CPV	
	Value	Uncertainty	Uncertainty	Difference
a (AU)	2.7653923855	2.7×10^{-9}	3.5×10^{-9}	7.8×10^{-9} (1.76 σ)
e	0.080018087	2.9×10^{-8}	3.5×10^{-8}	1.7×10^{-8} (0.37 σ)
i (deg)	10.5869052	3.4×10^{-6}	3.9×10^{-6}	2.4×10^{-6} (0.46 σ)
Ω (deg)	80.409725	1.9×10^{-5}	2.2×10^{-5}	4.9×10^{-5} (1.69 σ)
ω (deg)	73.235114	2.8×10^{-5}	3.4×10^{-5}	1.6×10^{-5} (0.36 σ)
M (deg)	124.513574	2.1×10^{-5}	2.6×10^{-5}	2.6×10^{-5} (0.78 σ)

Table 5 Accumulated |BC-405–CPV| state vector differences for NEA 2002 AT4

	epoch + 0.5 year	epoch + 1 year	epoch + 2 year	epoch + 5 year
x (m)	3.0	45	360	3600
y (m)	3.7	10	99	2500
z (m)	2.4	11	36	1100
\dot{x} (m/s)	5.7×10^{-7}	5.2×10^{-6}	2.4×10^{-5}	1.4×10^{-4}
\dot{y} (m/s)	5.2×10^{-8}	1.5×10^{-6}	1.0×10^{-5}	5.0×10^{-4}
\dot{z} (m/s)	1.5×10^{-7}	2.9×10^{-7}	1.2×10^{-6}	2.4×10^{-4}

2002 AT4 (estimated asteroid radius = 130 m, epoch = JD 2452315.5, barycentric equatorial reference frame).

Thus, while the BC-405 ephemeris was developed solely for this project, we suggest it may prove useful in other high-precision dynamical applications.

5 Future work

Among the limiting factors in astrometric mass determination is the precision of available observations.

For asteroid encounters that occur in the future, the introduction of systems like the Panoramic Survey Telescope & Rapid Response System (PanSTARRS) will help address this concern, with projected observational uncertainties at the 0.1 arcsecond level (Jedicke and The Pan-Starrs Collaboration 2004). Indeed, PanSTARRS could result in the discovery of several million main-belt bodies, providing a wealth of potential test asteroids.

For asteroid encounters that occurred in the past, we must necessarily use whatever observations were made; obtaining the most accurate and precise possible masses therefore requires realistically accounting for observational precision, bias, and correlation. As noted in Sect. 2.4, orbital analysts currently assume that all observations of a given minor planet are uncorrelated. But Carpino et al. (2003) have demonstrated that closely-spaced observations of an asteroid made by the same observatory are significantly correlated; ignoring this correlation has the effect of inaccurately weighting many observations in the least-squares algorithm. Additionally, the current assumption that all observatories in a given era have the same observational uncertainty is clearly unsatisfactory. Addressing these issues would require development of time-based error models for all contributing observatories, including models for the bias and RMS errors of each observatory, and a model for the correlation of observations. A first step in this direction has been taken by Carpino et al.; extension of this concept to all available optical asteroid observations will be our next task.

Finally, as noted in Sect. 2.4, each of the 56 valid mass determinations was made independently, with the determination of the orbit of a single test asteroid also yielding the mass of the perturbing subject asteroid. Ideally, we would like to simultaneously solve for all of the masses, as this would reveal correlations impacting the reliability of each result. Given the experience gained here, we plan to attempt this simultaneous solution, once the observational error models have been developed.

Acknowledgments The authors wish to thank E. Pitjeva and G. B. Valsecchi for kindly sharing the results of their previous work. This work was conducted in part at the Jet Propulsion Laboratory, California Institute of Technology, under a contract with the National Aeronautics and Space Administration.

References

- Baer, J.: Comet/asteroid orbit determination and ephemeris software. <http://www.home.earthlink.net/~jimbaer/> (2004). Accessed 18 Sep 2007
- Bange, J.: An estimation of the mass of asteroid 20-Massalia derived from the HIPPARCOS minor planets data. *Astron. Astrophys.* **340**, L1–L4 (1998)
- Bange, J.-F., Bec-Borsenberger, A.: Determination of the masses of minor planets. In: ESA SP-402: Hipparcos – Venice '97, pp. 169–172 (1997)
- Britt, D.T., Yeomans, D., Housen, K., Consolmagno, G.: Asteroid Density, Porosity, and Structure. In: Asteroids III Univ., Arizona Press, pp. 485–500 (2002)

- Carpino, M., Knezevic, Z.: Asteroid mass determination: (1) Ceres. In: Ferraz-Mello, S., Morando, B., Arlot, J.-E. (eds.) IAU Symposium 172: Dynamics, Ephemerides, and Astrometry of the Solar System, p. 203 (1996)
- Carpino, M., Milani, A., Chesley, S.R.: Error statistics of asteroid optical astrometric observations. *Icarus* **166**, 248–270 (2003)
- Carusi, A., Valsechi, G.B., Greenberg, R.: Planetary close encounters—Geometry of approach and post-encounter orbital parameters. *Celest. Mech. Dyn. Astr.* **49**, 111–131 (1990)
- Chernetenko, Y.A., Kochetova, O.M.: Masses of some large minor planets. In: Warmbein, B. (ed.) ESA SP-500: Asteroids, Comets, and Meteors: ACM 2002, pp. 437–440 (2002)
- Chesley, S.R., Owen, W.M. Jr., Hayne, E.W., Sullivan, A.M., Dumas, R.C., Giorgini, J.D., Chamberlin, A.B., Synnott, S.P., Vazquez, C.S.: The mass of asteroid 10 Hygiea. In: *Bulletin of the American Astronomical Society*, p. 524 (2005)
- Dunham, D.W., Dunham, J.B., Binzel, R.P., Evans, D.S., Freuh, M., Henry, G.W., A'Hearn, M.F., Schnurr, R.G., Betts, R., Haynes, H., Orcutt, R., Bowell, E., Wasserman, L.H., Nye, R.A., Giclas, H.L., Chapman, C.R., Dietz, R.D., Moncivais, C., Douglass, W.T., Parker, D.C., Beish, J.D., Martin, J.O., Monger, D.R., Hubbard, W.B., Reitsem, H.J., Klemola, A.R., Lee, P.D., McNamara, B.R., Maley, P.D., Manly, P., Markworth, N.L., Nolthenius, R., Oswalt, T.D. Smith, T.D. Strother, T.D. Povenmire, T.D. Purrington, T.D. Trenary, T.D. Schneider, T.D. Schuster, T.D. Moreno, T.D. Guichard, T.D. Sanchez, T.D. Taylor, T.D. Uppgren, T.D. von Flandern, T.D.: The size and shape of (2) Pallas from the 1983 occultation of 1 Vulpeculae. *AJ* **99**, 1636–1662 (1990)
- Giorgini, J.D., Chodas, P.W., Yeomans, D.K.: Horizons on-line ephemeris system. <http://www.ssd.jpl.nasa.gov/horizons.cgi> (1990). Accessed 1 Sep 2006
- Goffin, E.: The orbit of 203 Pompeja and the mass of Ceres. *Astron. Astrophys.* **249**, 563–568 (1991)
- Goffin, E.: New determination of the mass of Pallas. *Astron. Astrophys.* **365**, 627–630 (2001)
- Hilton, J.L.: US naval observatory ephemerides of the largest asteroids. *AJ* **117**, 1077–1086 (1999)
- Jedicke, R., The Pan-Starrs Collaboration: The Pan-STARRS solar system survey. In: 35th COSPAR Scientific Assembly. COSPAR, Plenary Meeting, vol. 35, p. 999 (2004)
- Kaasalainen, M., Torppa, J., Piironen, J.: Models of twenty asteroids from photometric data. *Icarus* **159**, 369–395 (2002)
- Kissling, W.M., Blow, G.L., Allen, W.H., Priestley, J., Riley, P., Daalder, P., George, M.: The diameter of 9 Metis from the occultation of SAO:190531. *Proc. Astron. Soc. Austr.* **9**, 150 (1991)
- Konopliv, A.S., Yoder, C.F., Standish, E.M., Yuan, D.-N., Sjogren, W.L.: A global solution for the Mars static and seasonal gravity, Mars orientation, Phobos and Deimos masses, and Mars ephemeris. *Icarus* **182**, 23–50 (2006)
- Krasinsky, G.A., Pitjeva, E.V., Vasilyev, M.V., Yagudina, E.I.: Hidden mass in the asteroid belt. *Icarus* **158**, 98–105 (2002)
- Kuzmanoski, M.: A method for asteroid mass determination. In: Ferraz-Mello, S., Morando, B., Arlot, J.-E. (eds.) IAU Symp. 172: Dynamics, Ephemerides, and Astrometry of the Solar System, p. 207 (1996)
- Kuzmanoski, M., Kovačević, A.: Motion of the asteroid (13206) 1997GC22 and the mass of (16) Psyche. *Astron. Astrophys.* **395**, L17–L19 (2002)
- Landgraff, W.: A determination of the mass of (704) Interamnia from observations of (993) Moultona. In: Ferraz-Mello, S. (eds.) Proceedings of IAU Symposium 152: Chaos Resonance and Collective Dynamical Phenomena in the Solar System, pp. 179–182. Kluwer, Dordrecht (1992)
- Lopez Garcia, A., Medvedev, Y.D., Morano Fernandez, J.A.: Using close encounters of minor planets for the improvement of their masses. In: Wytrzyszczak, I.M., Lieske, J.H., Feldman, R.A. (eds.) IAU Colloq. 165: Dynamics and Astrometry of Natural and Artificial Celestial Bodies, p. 199 (1997)
- Marchis, F., Descamps, P., Hestroffer, D., Berthier, J.: Discovery of the triple asteroidal system 87 Sylvia. *Nature* **436**, 822–824 (2005)
- Margot, J.L., Brown, M.E.: Discovery and characterization of binary asteroids 22 Kalliope and 87 Sylvia. In: *Bulletin of the American Astronomical Society*, p. 1133 (2001)
- Margot, J.L., Nolan, M.C., Benner, L.A.M., Ostro, S.J., Jurgens, R.F., Giorgini, J.D., Slade, M.A., Howell, E.S., Campbell, D.B.: Radar discovery and characterization of binary near-earth asteroids. In: Lunar and Planetary Institute Conference Abstracts. Lunar and Planetary Institute Conference Abstracts, vol. 33, p. 1849 (2002)
- Marsden, B.: Minor planet center orbit (MPCORB) database. <ftp://www.cfa-ftp.harvard.edu/pub/MPCORB/> (2005)
- Merline, W.J., Close, L.M., Dumas, C., Chapman, C.R., Roddier, F., Menard, F., Slater, D.C., Duvert, G., Shelton, C., Morgan, T.: Discovery of a moon orbiting the asteroid 45 Eugenia. *Nature* **401**, 565 (1999)
- Merline, W.J., Weidenschilling, S.J., Durda, D.D., Margot, J.L., Pravec, P., Storrs, A.D.: Asteroids do have satellites. In: Asteroids III, pp. 289–312 (2002)

- Michalak, G.: Determination of asteroid masses—I. (1) Ceres, (2) Pallas and (4) Vesta. *Astron. Astrophys.* **360**, 363–374 (2000)
- Michalak, G.: Determination of asteroid masses. II. (6) Hebe, (10) Hygiea, (15) Eunomia, (52) Europa, (88) Thisbe, (444) Ggyptis, (511) Davida and (704) Interamnia. *Astron. Astrophys.* **374**, 703–711 (2001)
- Michałowski, T., Kwiatkowski, T., Kaasalainen, M., Pych, W., Kryszczyńska, A., Dybczyński, P.A., Velichko, F.P., Erikson, A., Denchev, P., Fauvaud, S., Szabó, G.M.: Photometry and models of selected main belt asteroids I. 52 Europa, 115 Thyra, and 382 Dodona. *Astron. Astrophys.* **416**, 353–366 (2004)
- Milani, A., Chesley, S.R.: Asteroids—dynamics site. <http://www.hamilton.dm.unipi.it/cgi-bin/astdys/astibo> (1999)
- Neese, C.E.: Asteroid taxonomy. EAR-A-5-DDR-TAXONOMY-V5.0. NASA Planetary Data System (2005)
- Petit, J.-M., Durda, D.D., Greenberg, R., Hurford, T.A., Geissler, P.E.: The long-term dynamics of Dactyl's orbit. *Icarus* **130**, 177–197 (1997)
- Pitjeva, E.V.: Progress in the determination of some astronomical constants from radiometric observations of planets and spacecraft. *Astron. Astrophys.* **371**, 760–765 (2001)
- Pitjeva, E.V.: Estimations of masses of the largest asteroids and the main asteroid belt from ranging to planets, Mars orbiters and landers. In: 35th COSPAR Scientific Assembly, p. 2014 (2004)
- Pitjeva, E.V.: High-precision ephemerides of planets—EPM and determination of some astronomical constants. *Solar Sys. Res.* **39**, 176–186 (2005)
- Shepard, M.K., Margot, J.-L., Magri, C., Nolan, M.C., Schlieder, J., Estes, B., Bus, S.J., Volquardsen, E.L., Rivkin, A.S., Benner, L.A.M., Giorgini, J.D., Ostro, S.J., Busch, M.W.: Radar and infrared observations of binary near-Earth Asteroid 2002 CE26. *Icarus*, **184**, 198–210 (2006)
- Sitarski, G., Todorovic-Juchniewicz, B.: Determination of the mass of (1) Ceres from perturbations on (203) Pompeja and (348) May. *Acta Astron.* **42**, 139–144 (1992)
- Sitarski, G., Todorovic-Juchniewicz, B.: Determination of masses of Ceres and Vesta from their perturbations on four asteroids. *Acta Astron.* **45**, 673–677 (1995)
- Standish, E.M.: JPL Planetary and Lunar Ephemerides, DE405/LE405. Technical Report 312.F-98-048, JPL Interoffice Memorandum (1998)
- Standish, M.: Dynamical reference frame—current relevance and future prospects. In: Johnston, K.J., McCarthy, D.D., Luzum, B.J., Kaplan, G.H. (eds.) IAU Colloq. 180: Towards Models and Constants for Sub-Microarcsecond Astrometry, p. 120 (2000)
- Standish, E.M.: Masses of 1 Ceres, 2 Pallas, and 4 Vesta. Technical Report 312.F-01-006, JPL Interoffice Memorandum (2001)
- Standish, E.M., Newhall, X.X., Williams, J.G., Folkner, W.M.: JPL Planetary and Lunar Ephemerides, DE403/LE403. Technical Report 314.10-127, JPL Interoffice Memorandum (1995)
- Storrs, A.D., Dunne, C., Conan, J.-M., Mugnier, L., Weiss, B.P., Zellner, B.: A closer look at main belt asteroids 1: WF/PC images. *Icarus* **173**, 409–416 (2005)
- Tedesco, E.F., Noah, P.V., Noah, M., Price, S.D.: The supplemental IRAS minor planet survey. *AJ* **123**, 1056–1085 (2002)
- Thomas, P.C., Binzel, R.P., Gaffey, M.J., Storrs, A.D., Wells, E.N., Zellner, B.H.: Impact excavation on asteroid 4 Vesta: Hubble Space Telescope results. *Science* **277**, 1492–1495 (1997)
- Thomas, P.C., Parker, J.W., McFadden, L.A., Russell, C.T., Stern, S.A., Sykes, M.V., Young, E.F.: Differentiation of the asteroid Ceres as revealed by its shape. *Nature* **437**, 224–226 (2005)
- Torppa, J., Kaasalainen, M., Michałowski, T., Kwiatkowski, T., Kryszczyńska, A., Denchev, P., Kowalski, R.: Shapes and rotational properties of thirty asteroids from photometric data. *Icarus* **164**, 346–383 (2003)
- Valsecchi, G.B., Milani, A., Gronchi, G.F., Chesley, S.R.: Resonant returns to close approaches: Analytical theory. *Astron. Astrophys.* **408**, 1179–1196 (2003)
- Viateau, B.: Mass and density of asteroids (16) Psyche and (121) Hermione. *Astron. Astrophys.* **354**, 725–731 (2000)
- Viateau, B., Rapaport, M.: The orbit of (2) Pallas. *Astron. Astrophys. Suppl.* **111**, 305 (1995)
- Viateau, B., Rapaport, M.: Improvement of the orbits of asteroids and the mass of (1) Ceres. In: ESA SP-402: Hipparcos – Venice '97, p. 91–94 (1997a)
- Viateau, B., Rapaport, M.: The Bordeaux meridian observations of asteroids. First determination of the mass of (11) Parthenope. *Astron. Astrophys.* **320**, 652–658 (1997b)
- Viateau, B., Rapaport, M.: The mass of (1) Ceres from its gravitational perturbations on the orbits of 9 asteroids. *Astron. Astrophys.* **334**, 729–735 (1998)
- Viateau, B., Rapaport, M.: Mass and density of asteroids (4) Vesta and (11) Parthenope. *Astron. Astrophys.* **370**, 602–609 (2001)
- Vitagliano, A., Stoss, R.M.: New mass determination of (15) Eunomia based on a very close encounter with (50278) 2000CZ12. *Astron. Astrophys.* **455**, L29–L31 (2006)

- Williams, G.V.: The mass of (1) Ceres from perturbations on (348) May. In: Harris, A.W., Bowell, E. (eds.) *Asteroids, Comets, Meteors 1991*, pp. 641–643 (1992)
- Yeomans, D.K., Barriot, J.-P., Dunham, D.W., Farquhar, R.W., Giorgini, J.D., Helfrich, C.E., Konopliv, A.S., McAdams, J.V., Miller, J.K., Owen, W.M. Jr., Scheeres, D.J., Synnott, S.P., Williams, B.G.: Estimating the mass of asteroid 253 mathilde from tracking data during the NEAR flyby. *Science* **278**, 2106 (1997)
- Yeomans, D.K., Antreasian, P.G., Barriot, J.-P., Chesley, S.R., Dunham, D.W., Farquhar, R.W., Giorgini, J.D., Helfrich, C.E., Konopliv, A.S., McAdams, J.V., Miller, J.K., Owen, W.M., Scheeres, D.J., Thomas, P.C., Veverka, J., Williams, B.G.: Radio science results during the NEAR-shoemaker spacecraft rendezvous with eros. *Science* **289**, 2085–2088 (2000)